

## Transforming Discarded Mature Coconut Water into Carboxymethyl Cellulose as A Precursor Material for Bioplastics

Khusna Santika Rahmasari<sup>1\*</sup>, Achmad Vandian Nur<sup>1</sup>, Eka Anydia Putri<sup>1</sup>, Vanesa Maharani<sup>1</sup>, Achmad Ridlo<sup>2</sup>, Bayu Ishartono<sup>3</sup>

<sup>1</sup>Department of Pharmacy, Universitas Muhammadiyah Pekajangan Pekalongan, Pekalongan, 51172, Indonesia

<sup>2</sup>Pharmacy Vocational Program, Politeknik Kesehatan Kemenkes Surakarta, Klaten, 57425, Indonesia

<sup>3</sup>Department of Chemistry, Universitas Gadjah Mada, Sleman, 55281, Indonesia

\*Corresponding author: khusnasantika@gmail.com

### Abstract

Coconut vendors at the Traditional Market in Kedungwuni, Pekalongan Regency, often remove the discarded mature coconut water (DMCW) mixture into the market's drainage ditches after opening mature coconuts, resulting in soil contamination and odor due to acetic acid produced during fermentation by soil bacteria. This study aimed to minimize soil pollution caused by these activities through converting DMCW into versatile biopolymers such as carboxymethyl cellulose (CMC). The synthesis was initiated through the fermentation of DMCW into bacterial cellulose (BC) in the form of nata de coco (NdC), subsequently undergoing alkalization and carboxymethylation to produce CMC. The efficacy of the synthesis process from DMCW to CMC was identified via spectroscopy, thermal, and physicochemical analysis. The characterization results demonstrated that NdC-based CMC and commercial CMC exhibited analogous functional groups, diffraction patterns, thermal degradation behaviors, and physicochemical properties. NdC-based CMC revealed characteristics like water solubility, elevated molecular weight, and high viscosity, despite its purity being approximately 83.3%. Notwithstanding its rigidity, lack of transparency, and water solubility, this NdC-based CMC can be solvent cast into bioplastics and degraded in soil in four days. In the future, CMC-based bioplastics, enhanced through advanced treatments, will be expected as precursors for the creation of sustainable food packaging materials.

### Keywords

DMCW, NdC, CMC, Physicochemical Properties, Bioplastics

Received: 28 December 2024, Accepted: 8 April 2025

<https://doi.org/10.26554/sti.2025.10.3.698-711>

## 1. INTRODUCTION

A market is the hub of economic activity where buyers and sellers cross to engage in exchanges involving products and services. Conventional markets in rural areas create an interesting phenomenon whereby coconut sellers handle mature coconut water and also provide coconut grating services. Coconuts are regarded as a significant food source and a commodity with substantial economic worth in various facets of daily life. In traditional markets like Kedungwuni Market in Pekalongan Regency, coconut vendors who also serve as coconut graters play an important role in providing both young and mature coconuts, as well as processed products like young coconut water and shavings, grated mature coconut, coconut milk, and even coconut oil. However, the coconut grating process creates a byproduct in the form of mature coconut water, which is frequently discarded in large quantities. This discarded mature coconut water (DMCW) was reported to be abundant in nutrients, including protein, fat, and carbohydrates, with total

sugars comprising fructose, glucose, and sucrose, presenting potential value-added opportunities (Aba et al., 2024).

Nevertheless, it was frequently underutilized and ultimately becomes waste. DMCW produced by the grating of coconut meat was commonly discarded in backyards or front drainage ditches, causing unpleasant odors and polluting the soil and water sources. According to literature reviews, the untreated disposal of mature coconut water into the environment resulted in the production of acetic acid odors caused by soil bacterial fermentation (Detudom et al., 2023). The presence of acetic acid resulting from the fermentation of DMCW can lower soil pH, potentially affecting soil fertility (Kong et al., 2022). Therefore, it is crucial to discover new approaches for regulating DMCW to mitigate its environmental pollution impacts. These creative ventures are expected to provide new, eco-friendly, and more sustainable goods while enhancing the value of DMCW.

To address the aforementioned issues while also developing an innovative product, this study offered a problem-solving

approach by implementing biotechnological processes. It involved the total sugar content in DMCW, frequently discarded by coconut traders and shredders at Kedungwuni Market, Pekalongan Regency. A processed product obtained from DMCW through biotechnological methods is bacterial cellulose (BC), typically known as nata de coco (NdC). NdC is a natural hydrogel consisting of a three-dimensional framework of irregularly shaped bacterial cellulose, facilitated by the starter bacterium *Acetobacter xylinum* (Phan et al., 2023). NdC is a form of bacterial cellulose (BC) that exhibits enhanced physicochemical properties, including high purity, degree of polymerization, crystallinity, tensile strength, water retention capacity, and exceptional biocompatibility (Rachtanapun et al., 2021). Organoleptically, NdC is chewy and transparent, making it a popular fiber-rich food ingredient. Previous work has spectrometrically documented the increased cellulose content in NdC, revealing distinct diffraction peaks of crystalline cellulose at  $2\theta = 14.5, 16.8, \text{ and } 22.8^\circ$  (Phan et al., 2023). NdC is primarily employed as food sources and have also been utilized as dye adsorbents (Phan et al., 2023), edible coatings for fruits (Techavuthiporn et al., 2024), hydrogels (Halib et al., 2010), cell culture substrates (Luo et al., 2019), tissue engineering materials (Nimeskern et al., 2013), and in the creation of cellulose derivative biopolymers (Rachtanapun et al., 2021). However, investigation into the utilization of NdC's enhanced cellulose content for derivative products with innovative and diverse benefits remains limited.

NdC, rich in cellulose, underwent sophisticated molecular chemical engineering through alkalization and carboxymethylation processes to produce a final cellulose-derived product, namely carboxymethyl cellulose (CMC) biopolymer. CMC is an anionic polysaccharide derivative of cellulose that is water-soluble, non-toxic, easily degraded by soil microbes, has a high molecular weight, and can be used as a binder reinforcement due to its molecular properties, forming a colloidal system with high viscosity (Lakshmi et al., 2017; Techavuthiporn et al., 2024). Previous study has demonstrated that CMC was extensively utilized as an edible food coating, in the development of food packaging, and as active food packaging, all of which primarily rely on commercial CMC (Andrade et al., 2022; Du et al., 2023; Ramakrishnan et al., 2024). Currently, commercially accessible CMC from various chemical suppliers is considered to have limitations, including lengthy ordering processes and high expenses. This means effort to fabricate CMC from biomass resources and their derivatives is recognized as an intriguing challenge in offering an alternative biopolymer. Recent study has shown that CMC can be successfully synthesized from NdC in fresh coconut water with the addition of pro-analyst reagents such as di-ammonium hydrogen orthophosphate, magnesium sulfate, and citric acid (Rachtanapun et al., 2021). Furthermore, CMC have been successfully synthesized from biomass sources including corn husks (Mondal et al., 2015), corn cobs (Shui et al., 2017), seaweed (Lakshmi et al., 2017), office paper waste (Wongvitvichot et al., 2021), water hyacinth (Saputra et al., 2014), sugarcane bagasse (Ge and

Li, 2013), and banana stems (Adinugraha et al., 2005). This work proposed fabricating CMC from NdC utilizing DMCW, which has been modified with food-grade chemical reagents, as introducing a distinct feature while mitigating the adverse effects of DMCW disposal in the Kedungwuni's traditional market, Pekalongan Regency.

Efforts to reduce environmental pollution while simultaneously creating creative, eco-friendly, and sustainable goods, as well as increasing the value of DMCW, will be carried out through the synthesis and characterization of CMC generated from DMCW-based NdC. This study investigated the synthesis of DMCW-based NdC utilizing food-grade chemical reagents. Subsequently, the NdC will undergo alkalization and carboxymethylation to produce CMC, with the success of the synthesis confirmed using spectroscopic analysis. The physicochemical properties, including the degree of substitution (DS), viscosity, molecular weight (Mw), final CMC content, water and oil resistance capacity, proximate analysis, density, color testing of CMC, NaCl content, sodium glycolate content, and heavy metal ion content, along with its application as a bioplastic precursor, will be discussed in more detail in this study.

## 2. EXPERIMENTAL SECTION

### 2.1 Materials

The DMCW derived from the blending of multiple mature coconuts was obtained from a coconut vendor at the Traditional Market in Kedungwuni, Pekalongan Regency, Central Java. The starter bacteria *Acetobacter xylinum* and foodgrade ammonium sulfate ((NH<sub>4</sub>)<sub>2</sub>SO<sub>4</sub>) were obtained from Nata de Coco Indohasco, a local supplier in Nganjuk Regency, East Java. The chemicals utilized in this study were manufactured by Merck and employed directly without further purification, including glacial acetic acid (CH<sub>3</sub>COOH) (CAS No. 64-19-7), sodium hydroxide (NaOH) (CAS No. 1310-73-2), monochloroacetic acid (MCA) (ClCH<sub>2</sub>COOH) (CAS No. 79-11-8), isopropanol (CH<sub>3</sub>CH(OH)CH<sub>3</sub>) (CAS No. 67-63-0), hydrochloric acid 37% (HCl) (CAS No. 7647-01-0), silver nitrate (AgNO<sub>3</sub>) (CAS No. 7761-88-8), sodium chloride (NaCl) (CAS No. 7647-14-5), acetone (CH<sub>3</sub>COCH<sub>3</sub>) (CAS No. 67-64-1), nitric acid (HNO<sub>3</sub>) 65% (CAS No. 7697-37-2), phenolphthalein (C<sub>20</sub>H<sub>14</sub>O<sub>4</sub>) (CAS No. 77-09-8), absolute methanol (CH<sub>3</sub>OH) (CAS No. 67-56-1), absolute ethanol (CH<sub>3</sub>CH<sub>2</sub>OH) (CAS No. 64-17-5), and thioglycolic acid (HSCH<sub>2</sub>COOH) (CAS No. 68-11-1). Additional chemicals utilized in this study, manufactured by Sigma-Aldrich with pro-analysis quality, including standard CMC (CAS No. 9004-32-4) and 2,7-dihydroxynapht halene (C<sub>10</sub>H<sub>6</sub>(OH)<sub>2</sub>) (CAS No. 582-17-2). Other supporting materials used in this study included distilled water (CV. Brataco), commercial sucrose (local store in Kedungwuni), olive oil (Fresh Pomace), and prepackaged organic planting medium fortified with *Trichoderma* fungi (Infarm.id Official Shop).

### 2.2 Characterization

Functional groups were identified using the Spirit QATR-S Shimadzu Infrared (IR) spectrometer with attenuated total

reflectance (ATR) instrument at a wavelength of 400-4000  $\text{cm}^{-1}$ . The Shimadzu Maxima XRD-7000 X-Ray Diffractometer recorded the diffraction pattern with a  $2\theta$  angle range of 10 to  $90^\circ$ , a scan rate of  $2^\circ/\text{min}$ , and a  $\text{CuK}\alpha$  radiation tube ( $\lambda = 1.54 \text{ \AA}$ ; 40.0 kV; 30.0 mA). The thermal properties of synthesised NdC, CMC, and CMC-based bioplastics were examined utilising a Linseis STA PT1600 DTA-TGA instrument. The analysis was performed at temperatures ranging from 30 to  $600^\circ\text{C}$ , utilising a heating rate of  $10^\circ\text{C}/\text{min}$  and a water flow rate of 0.5 L/min. The absorbance data analysis to assess the physicochemical properties of the synthesised material was conducted using a Shimadzu UV-1280 UV-visible spectrophotometer.

### 2.3 Synthesis of DMCW-Based NdC

The synthesis of DMCW-based NdC was performed utilizing a modified reference method from the local supplier of NdC, Nata de Coco Indohasco. Briefly, the synthesis of DMCW-based NdC involved filtering and heating 1 L of DMCW, subsequently adding 100 g of commercial sucrose. After cooling, 10 mL of glacial acetic acid, 10 g of food-grade ammonium sulfate, and 100 mL of *Acetobacter xylinum* starter culture were added to the container and covered with newspaper. NdC was harvested after a 10-day fermentation process, followed by preparation stages that included cutting it into smaller pieces, washing it five times, and heating it in an oven at  $55^\circ\text{C}$  until its mass stabilized. The final dried NdC was ground and sieved through a 60-mesh sieve before moving on to further processing and characterization. NdC was characterized using ATR-IR, XRD, organoleptic tests, proximate analysis, and thermal properties.

### 2.4 Synthesis of NdC-Based CMC

The synthesis of NdC-based CMC was conducted through alkylation and carboxymethylation methods, which were adapted from existing references with further modifications (Rachtanapun et al., 2021). Fine NdC powder (Figure 1b), with a particle size of 60 mesh, was immersed with 15 mL of NaOH solutions at varying concentrations (10, 20, 30, 40, and 50%) and 30 mL of isopropanol (IPA), while stirring for 30 min. Different quantities of monochloroacetic acid (MCA) solids (1.5, 3.0, 4.5, 6.0, and 7.5 g) were incorporated into the mixture to activate the carboxymethylation reaction. The procedure was conducted with continuous stirring and heating at  $55^\circ\text{C}$  for a duration of 30 min. The solid phase was subsequently separated from the liquid phase and washed with 20 mL of absolute methanol, followed by neutralization with 80% glacial acetic acid. The solid underwent additional washing with technical ethanol via a Buchner filter five times, followed by oven drying at  $60^\circ\text{C}$  until a constant mass was achieved. The final product, CMC, was analyzed using organoleptic testing, proximate analysis, ATR-IR, XRD, DTA-TGA, and physicochemical methods.

## 2.5 Determination of Physicochemical Properties

### 2.5.1 Degree of Substitution (DS)

DS was assessed through a titration method, following established references with minor modifications (Lakshmi et al.,

2017). In the preparation stage, 0.2 g of synthesized CMC and commercial CMC from Sigma-Aldrich, respectively, were suspended in a mixture of 15 mL absolute ethanol and 1 mL of  $\text{HNO}_3$  2M. The suspension was agitated and heated to  $50^\circ\text{C}$  for a duration of 10 min. Following heating, the solid phase was isolated via a Buchner funnel, subjected to five washes with absolute methanol, and subsequently dried in an oven at  $100^\circ\text{C}$  for 3 h until a constant mass was attained. During the titration stage, 100 mg of each prepared CMC sample was dissolved in distilled water, after which 5 mL of NaOH 0.3M and 2-3 drops of phenolphthalein solution were added. The mixture underwent titration using a 0.3M HCl solution. A blank solution was prepared by adding 5 mL of NaOH 0.3M and 2-3 drops of phenolphthalein solution, which was subsequently titrated with HCl 0.3M. The volume of HCl ( $V_n$ ) utilized in the titration was recorded, and each titration was conducted three times to ensure accuracy. The carboxymethyl content (CM) and DS were determined in succession using Equations (1) and (2).

$$\text{Carboxymethyl content (\%CM)} = \frac{[(V_o - V_n)M \times 0.059 \times 100]}{m} \quad (1)$$

$$\text{DS} = \frac{162 \times (\%CM)}{5900 - (58 \times (\%CM))} \quad (2)$$

where  $V_o$  denote the volume of HCl utilized for blank titration (mL), M indicate the concentration of HCl (M), and m represent the mass of CMC (g).

### 2.5.2 Determination of Viscosity, Molecular Weight (Mw), and Final CMC Content

The viscosity of the synthesized CMC and the commercial CMC from Sigma-Aldrich, both at a 4% concentration and measured at  $25^\circ\text{C}$ , was evaluated using a Brookfield DV2T viscometer. The Mw of both CMC variants was assessed via TOSOH HLC-8320 Gel Permeation Chromatography (GPC) instrument. The ultimate CMC content was established using an enhanced reference technique (Mondal et al., 2015). In this procedure, 0.15 g of synthesized CMC was merged with 20 mL of 80% methanol, agitated for 10 min, thereafter filtered, and rinsed utilizing absolute methanol in a Buchner filter. The final CMC content was determined by Equation (3).

$$\text{Final CMC content (\%)} = \frac{m}{m_0} \times 100\% \quad (3)$$

Here, m refers to the mass of CMC post-washing (g), while  $m_0$  indicates the mass of CMC before the washing process (g).

### 2.5.3 Water and Oil Retention Capacity

The assessment of water retention capacity (WRC) and oil retention capacity (ORC) was performed using a modified process based on a cited method (Mondal et al., 2015). Each 0.1

g of synthetic CMC powder and standard CMC from Sigma-Aldrich was mixed in 20 mL of either olive oil or distilled water in centrifuge tubes. The mixes were incubated in a water bath at 40 °C for 30 min. The materials were subsequently centrifuged for 15 min to achieve separation into two different layers. The precipitate was gathered and weighed to get the WRC and ORC values.

#### 2.5.4 Analysis of Proximate, Density, and Color

A proximate analysis was conducted on NdC, NdC-derived CMC, and commercially available CMC from Sigma-Aldrich. The analysis encompassed assessments of moisture, ash, protein, and fat contents. The moisture content was evaluated using gravimetric methods with an oven maintained at 105 °C for 3 h. Ash content was assessed utilizing porcelain crucibles and a muffle furnace, with samples burned at 600 °C. The protein content was quantified using the Kjeldahl method with a Digestion System from Behr GmbH, Germany. Fat content was extracted utilizing the Soxhlet technique with a FOSS Fat Extraction Unit (Soxtec ST243). Density measurements were conducted using a pycnometer at room temperature, while color parameters ( $L^*$ ,  $a^*$ ,  $b^*$ ) were evaluated with an AMT511 colorimeter.

#### 2.5.5 Determination of NaCl Content

The quantification of NaCl content was conducted utilizing a modified approach derived from a reference (Mondal et al., 2015). Each 0.2 g of synthetic and Sigma-Aldrich standard CMC was diluted in 20 mL of methanol 65% and then stored in a sealed container for 3 h. A 10 mL portion of the mixture was subsequently neutralized to pH 7 with a 0.1 M  $\text{HNO}_3$  solution. The NaCl concentration was ascertained by titrating the mixture with a 0.1 M  $\text{AgNO}_3$  solution and computed using Equation (4).

$$\text{NaCl content (\%)} = \frac{1.461 \times V}{m} \quad (4)$$

where V represents the volume of  $\text{AgNO}_3$  utilized (mL) and m denotes the dry mass of CMC (g).

#### 2.5.6 Determination of Sodium Glycolate Content

The sodium glycolate concentration was determined using a modified method based on a reference (Mondal et al., 2015). In total, 0.25 g of synthetic CMC and 0.25 g of Sigma-Aldrich standard CMC were dissolved in 5 mL of glacial acetic acid and 5 mL of distilled water, respectively. Subsequently, 25 mL of acetone and 0.5 g of NaCl were added into each solution while stirring until precipitation ensued. The mixes underwent centrifugation, and the resultant clear filtrate was utilized for absorbance measurement. A blank solution was made by combining 5 mL of glacial acetic acid with 5 mL of distilled water, 25 mL of acetone, and 0.5 g of NaCl. Subsequently, each solution was combined with 10 mL of a 1% 2,7-dihydroxynaphthalene solution, and its absorbance was recorded at a wavelength of 540 nm utilizing a Shimadzu UV-1280 UV-visible spectrophotometer. A calibration curve was

created utilizing thioglycolic acid solutions combined with 10 mL of acetone, encompassing a concentration range of 1, 2, 3, 4, and 5 ppm. The sodium glycolate concentration was ascertained utilizing Equation (5).

$$\text{Sodium glycolate content (\%)} = \frac{a \times 1.29}{b} \quad (5)$$

In this context, 1.29 denotes the conversion factor from glycolic acid to sodium glycolate, a signifies the amount of glycolic acid derived from the standard curve (mg), and b indicates the mass of the CMC powder (g).

#### 2.5.7 Analysis of Heavy Metal Ions

Analysis of heavy metal ions was performed to identify Pb, Cd, Fe, and Cr ions both qualitatively and quantitatively, employing the Shimadzu AA-7800 Series Atomic Absorption Spectrophotometer (AAS) with flame analysis, supplemented by microwave digestion for the preparation of solid samples.

### 2.6 CMC-Based Film Preparation

Films derived from synthetic CMC and commercially sourced CMC from Sigma-Aldrich were fabricated using the solvent casting process, following protocols outlined in pertinent studies (Rahmasari and Ishartono, 2024). Synthesized and commercial CMC, in quantities of 200, 300, and 400 mg, were dissolved in 10 mL of distilled water while being stirred and heated concurrently. After achieving a uniform mixture, it was put into glass molds with a diameter of 6 cm and dried at 60 °C in an oven to make bioplastics. The bioplastics were further studied via ATR-IR and XRD spectroscopy, evaluated for their physicochemical properties, and examined for biodegradability.

#### 2.7 Physicochemical Properties of CMC-Based Bioplastics

The physicochemical properties of CMC-based bioplastics involved the evaluation of many parameters, including mechanical tests (tensile strength (TS) and elongation (E), transmittance, water solubility, and biodegradability assessment. The mechanical qualities, namely TS and E, were assessed utilizing a Zwick 0.5 Universal Testing Machine (UTM). Transmittance analysis was conducted using a Shimadzu UV-1280 UV-visible spectrophotometer at a wavelength of 660 nm, adhering to recognized reference methodologies (Rachtanapun et al., 2021). The water solubility test entailed sectioning bioplastic samples into 2×2 cm pieces, measuring their weight, and submerging them in 50 mL of distilled water. The biodegradability was assessed by the soil burial test method, wherein intact bioplastic samples, measuring 6 cm in diameter, were pre-weighed and subsequently buried in a container filled with humus-rich soil that included *Trichoderma* fungi. Biodegradability test observations were performed on days 1, 2, 3, and 4 post-burials (Rahmatullah et al., 2022).

**Table 1.** Comparative Study of Proximate Results for DMCW-Based NdC, NdC-Based CMC, and Commercial CMC

Parameters/Samples	Moisture content (%)	Ash content (%)	Protein content (%)	Fat content (%)	Reference
DMCW-based NdC	2.00	35.10	12.57	0.41	This study
NdC-based CMC	0.50	11.68	1.30	0.03	This study
Sigma-Aldrich standard CMC	1.00	8.55	0.11	0.04	This study
Corn husk-based prepared CMC	2.21	18.05	Not provided	Not provided	(Mondal et al., 2015)
Baobab fruit shell-based CMC	5.57	2.62	Not provided	Not provided	(Youssif and Hassan, 2018)
Banana peel-based CMC	11.96	1.93	Not provided	Not provided	(Alabi et al., 2020)

### 3. RESULTS AND DISCUSSION

#### 3.1 Synthesis and Characterization of DMCW-Based NdC and NdC-Based CMC

The DMCW-based NdC (Figure 1a) and NdC-based CMC (Figure 1c) produced in this work were assessed using organoleptic and physicochemical studies. In general, and as evidenced by a review of the literature from previous research, the chemical composition of DMCW was comprised sugars such as glucose, fructose, and sucrose; essential minerals in the form of cations, including Na, Ca, K, and Fe; vitamins such as riboflavin (B2), niacin (B3), pyridoxine (B6), and ascorbic acid (C); and total carbohydrates, fats, proteins, and water (Aba et al., 2024). *Acetobacter xylinum* converted the sugars in DMCW to produce NdC and acetic acid as a by-product. The NdC produced from the fermentation of DMCW with *Acetobacter xylinum* starter displayed a primarily white appearance with a subtle brownish hue. The DMCW-based NdC exhibited a neutral or mildly acidic scent and flavor as a result of fermentation activity. The NdC-based CMC, resulting from the alkalization and carboxymethylation of NdC, was identified as a solid powder that passes through a 60-mesh screen, primarily white with a subtle brownish hue. Figure 1 depicted both synthesized products from this work. Quantitatively, the fermentation process of 1 L of DMCW generated 502.31 g of wet DMCW-based NdC (Figure 1a), which was subsequently converted to its dry form (Figure 1b), yielding 25.91 g. The significant mass reduction was a consequence of the heating process in the oven carried out prior to the conversion of the DMCW-based NdC material into NdC-based CMC, which resulted in the loss of water molecules that are bound within the material. The thermogram in Figure 4 provided additional information regarding the water content loss. Furthermore, the alkalization and carboxymethylation processes converted the entire mass of dry DMCW-based NdC into NdC-based CMC, resulting in a 95.67% conversion (Figure 1c).

Additionally, the proximate analysis results, including moisture, ash, protein, and fat content of DMCW-based NdC, NdC-based CMC, and commercial CMC (Sigma-Aldrich), were pre-

sented in Table 1. The proximate test findings, including moisture content, ash, protein, and fat levels, for DMCW-based NdC compared to NdC-based CMC demonstrated a declining trend. This trend indicated that the elevated carbohydrate content, particularly total sugars (glucose, fructose, and sucrose), protein, and fat in DMCW (Aba et al., 2024) was effectively transformed into DMCW-based NdC via a fermentation process mediated by *Acetobacter xylinum*. The notable decrease in proximate values of DMCW-based NdC relative to NdC-based CMC was also ascribed to the participation of alkalization reactions utilizing NaOH and carboxymethylation with MCA. Moreover, the proximate values of NdC-based CMC were determined to be analogous to those of commercially available CMC from Sigma-Aldrich. Consequently, the synthesis process converting DMCW into NdC and subsequently into CMC can be deemed successful based on organoleptic and proximate analytical outcomes.

The efficacy of the synthesis procedure for DMCW-based NdC and NdC-based CMC was assessed by organoleptic and proximate testing, as well as spectroscopic examination. Figure 2 displayed the ATR-IR characterization results for DMCW-based NdC, NdC-based CMC, and commercial CMC from Sigma-Aldrich. The spectra in Figure 2 demonstrated comparable patterns among DMCW-based NdC (Figure 2a), NdC-based CMC (Figure 2b), and Sigma-Aldrich commercial CMC (Figure 2c), despite notable discrepancies in the attenuation of functional group absorption intensities. The absorption bands at wavenumbers 3270-3332  $\text{cm}^{-1}$  were attributed to O-H stretching vibrations (Techavuthiporn et al., 2024). The bands at 2930-2916  $\text{cm}^{-1}$  signified C-H stretching vibrations from methylene groups ( $-\text{CH}_2$ ) (Roslan et al., 2024; Techavuthiporn et al., 2024). The diminished strength of these bands in DMCW-based NdC relative to NdC-based CMC was likely attributable to the influences of alkalization and carboxymethylation processes. The displacement of the absorption band linked to carbonyl (C=O) stretching vibrations at 1630  $\text{cm}^{-1}$  (Techavuthiporn et al., 2024) was ascribed to carboxymethylation reactions involving MCA on DMCW-based NdC, resulting in a new ab-

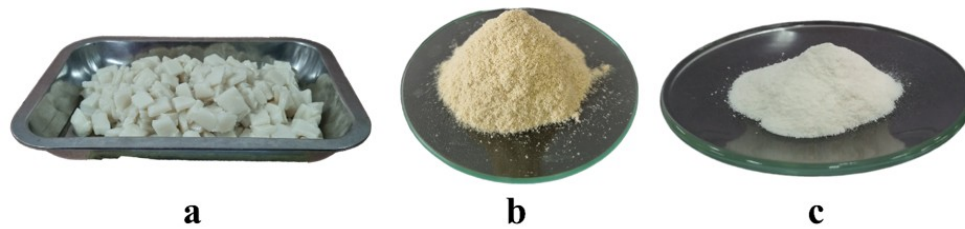


**Figure 1.** Final Product of DMCW-Based NdC (a), Fine Powder of NdC (b), and NdC-Based CMC (c)

sorption band at  $1588\text{ cm}^{-1}$ , which corresponds to carboxyl group ( $-\text{COO}^-$ ) vibrations in NdC-based CMC (Wongvitvichot et al., 2021). Absorptions at  $1428$  and  $1414\text{ cm}^{-1}$  revealed  $-\text{CH}_2$  bending vibrations, as demonstrated in the spectra of both Figure 2a and Figure 2b (Wongvitvichot et al., 2021). The bands at  $1317$ - $1322\text{ cm}^{-1}$  indicated the presence of C-H bending vibrations (Roslan et al., 2024). Sharp peaks at  $1026$ - $1017\text{ cm}^{-1}$  were suggested of the stretching vibrations of  $\text{HOC}-\text{O}-\text{CH}_2$  (Lakshmi et al., 2017). Based on infrared spectrometric examination, the alkalization and carboxymethylation processes were proven to successfully transform DMCW-based NdC into NdC-based CMC, as evidenced by the IR spectra's similarity to that of Sigma-Aldrich's commercial CMC.

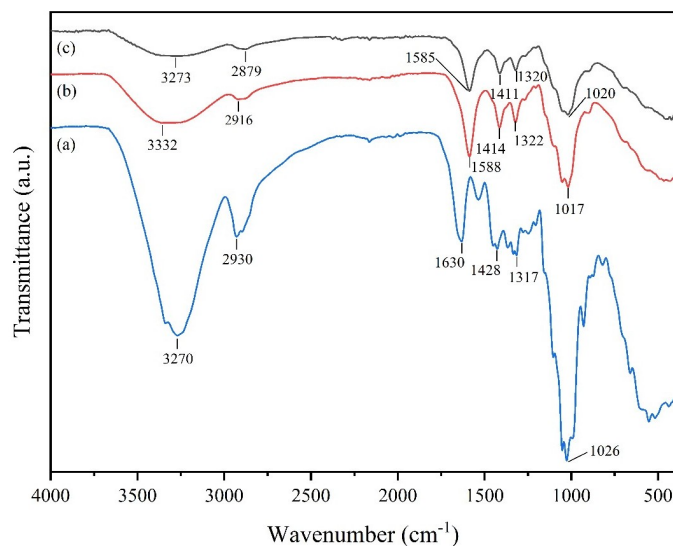


**Figure 2.** Infrared Spectra of DMCW-Based NdC (a), NdC-Based CMC (b), and Sigma-Aldrich Standard CMC (c)

The X-ray diffraction patterns shown in Figure 3 demonstrated the synthesis process's success in creating DMCW-based NdC and NdC-based CMC. Figure 3a displayed that the XRD pattern of DMCW-based NdC exhibits prominent crystalline cellulose peaks at  $2\theta = 14.7^\circ$  (101),  $16.9^\circ$  (10-1),  $22.8^\circ$  (002),  $44.0^\circ$ ,  $64.3^\circ$ , and  $77.4^\circ$  (Kumar et al., 2020; Lakshmi et al., 2017; Phan et al., 2023; Wongvitvichot et al.,

2021). The increased crystallinity noted in DMCW-based NdC was attributable to the cellulose structure generated during fermentation facilitated by *Acetobacter xylinum*. In contrast, the NdC-based CMC pattern in Figure 3b revealed an amorphous characteristic, resulting from the deterioration of the crystalline cellulose structure in DMCW-based NdC (Mondal et al., 2015; Wongvitvichot et al., 2021). The treatment of DMCW-based NdC with NaOH induced swelling in the cellulose structure, resulting in an increase in surface area and accessibility of hydroxyl ( $-\text{OH}$ ) groups on the cellulose chains. Additionally, it resulted to the partial removal of intramolecular and intermolecular hydrogen bonds within the cellulose, rendering it more amorphous. This disruption allowed the integration of active groups from MCA, substituting hydrogen atoms and culminating in the production of NdC-based CMC as the final product. The XRD pattern of NdC-based CMC and commercial CMC from Sigma-Aldrich (Figure 3c) were similar, indicating that the synthesis method was successful.

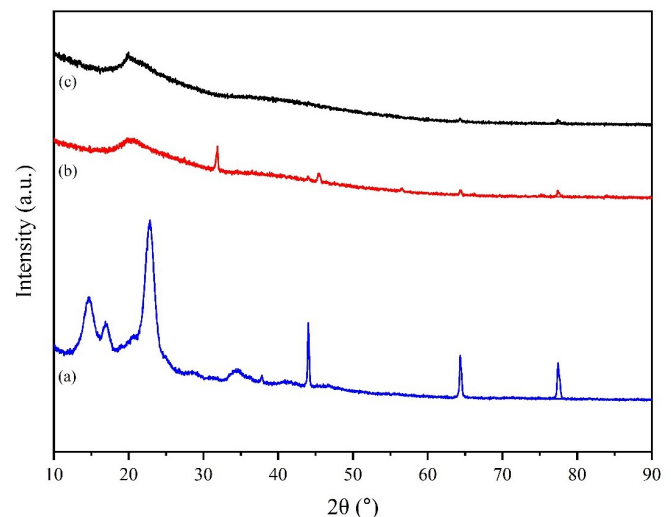


**Figure 3.** Diffraction Pattern of DMCW-Based NdC (a), NdC-Based CMC (b), and Sigma-Aldrich Standard CMC (c)

The thermogram in Figure 4 provided supplementary characterization to validate the successful synthesis of DMCW-based NdC and NdC-based CMC, in conjunction with organoleptic, proximate, and spectroscopic investigations. The thermo-

gram of DMCW-based NdC (Figure 4a) indicated two phases of thermal deterioration, occurring below 140 °C and between 260-550 °C. The thermal degradation occurring below 140 °C was ascribed to the loss of water molecules present in the DMCW-based NdC material (Table 1 in moisture content). The thermal degradation trend identified between 260-550 °C signified the deterioration of the crystalline cellulose framework within the DMCW-based NdC structure (Wongvitvichot et al., 2021). The thermogram of NdC-based CMC (Figure 4b) displayed a three-stage thermal degradation pattern within the temperature ranges of 50-115, 265-295, and 510-600 °C. A mass loss of 1.40% during the temperature range of 50-115 °C was ascribed to the evaporation of water molecules associated with the NdC-based CMC structure (Table 1 in moisture content). The thermal deterioration occurring between 265-295 °C, resulting in a 35.15% mass loss, was presumably attributable to the liberation of carboxylate groups as carbon dioxide (CO<sub>2</sub>) gas or the cleavage of hydroxymethyl groups (-CH<sub>2</sub>-OH) (Lakshmi et al., 2017; Wongvitvichot et al., 2021). The thermal degradation trend noted between 510-600 °C, resulting in a 15.20% mass loss, was ascribed to the deterioration of the polymer backbone originating from the six-membered pyranose ring structure (Lakshmi et al., 2017). The supporting evidence indicated that the thermal degradation temperature of NdC-based CMC was less compared to the DMCW-based NdC. This phenomenon was the result of the alkalization process with NaOH, which disrupts the crystallinity of cellulose, and the subsequent substitution with carboxylate groups from MCA. These two elements markedly lower the breakdown temperature in comparison to native cellulose (Wongvitvichot et al., 2021). Furthermore, the thermogram of commercial CMC from Sigma-Aldrich (Figure 4c) exhibited enhanced thermal degradation characteristics relative to NdC-based CMC. This was ascribed to the impact of its elevated molecular weight and DS (Wongvitvichot et al., 2021).

### 3.2 Analysis of Physicochemical Properties

#### 3.2.1 Analysis of DS

This study provides the physicochemical characterization of DMCW-based NdC and NdC-based CMC products, encompassing the analysis of DS, viscosity, Mw, final CMC content, WRC, ORC, density, color, NaCl content, sodium glycolate content, and heavy metal ions. DS represents the quantity of hydroxyl groups (-OH) replaced by carboxymethyl groups (-CH<sub>2</sub>COOH) on the carbon chains at locations C2, C3, or C6 (Rachtanapun et al., 2021; Wongvitvichot et al., 2021). The DS values for NdC-based CMC produced with different amounts of NaOH concentration and MCA mass were illustrated in Figures 5 and 6. Figure 5 depicted a pattern of escalating DS values to an optimal point (0.88 ± 0.02). This trend was ascribed to elevated NaOH concentrations, which augment the ionization of cellulose hydroxyl groups, resulting in the formation of more reactive alkoxide groups (RO<sup>-</sup>) that readily engage with substitution agents such as MCA. A sufficiently elevated NaOH concentration provided a basic re-

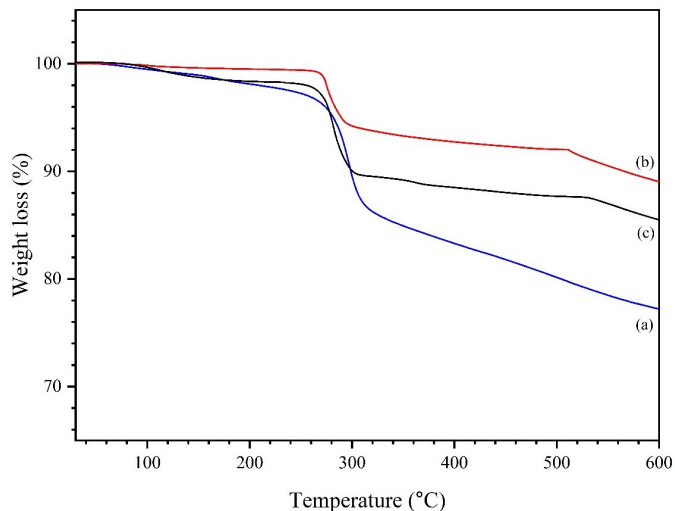


**Figure 4.** Thermal Gravimetry Analysis of DMCW-Based NdC (a), NdC-Based CMC (b), and Sigma-Aldrich Standard CMC (c)

action environment, promoting the etherification reaction with MCA. However, the DS value drops ( $0.86 \pm 0.01$ ) when the NaOH concentration increased above 50%. This was probably because cellulose broke down through an alkaline depolymerization process, which reduced the cellulose chain length and led to fewer hydroxyl groups available for replacement. Moreover, high concentrations of NaOH could initiate the production of by-products like sodium glycolate, thereby diminishing the substitution efficiency of MCA (Rachtanapun et al., 2021; Wongvitvichot et al., 2021).

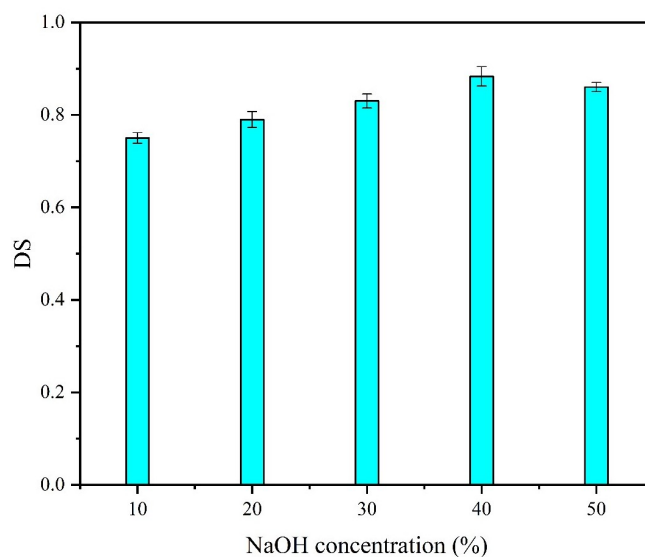


**Figure 5.** The Influence of NaOH Concentration on DS

In accordance with the trend of rising DS values noted in the prior discussion regarding NaOH concentration, Figure

6 similarly depicted the increase in DS values resulting from the addition of MCA mass. The DS value achieved its peak ( $0.88 \pm 0.02$ ) for a particular MCA mass before decreasing with an MCA mass change of 7.5 g. This process was caused by the incorporation of MCA, which enhanced the concentration of reactive molecules in the DMCW-based NdC combination with NaOH, thereby augmenting the likelihood of interactions between MCA and hydroxyl groups in cellulose. Nevertheless, beyond the optimal situation, an excessive quantity of MCA did not substantially enhance the DS value. This restriction depended on the limited availability of hydroxyl groups for substitution reactions and the possible generation of byproducts, including unreacted sodium salts of MCA (Rachtanapun et al., 2021; Wongvitvichot et al., 2021).

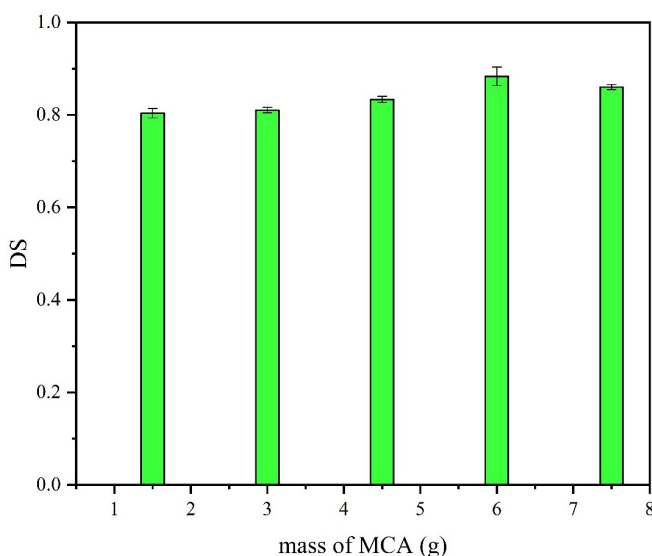


**Figure 6.** The Influence of MCA Mass on DS

The solubility properties of NdC-based CMC in water were influenced by its DS value. As the DS value increased, the solubility of NdC-based CMC in water also improved (Lakshmi et al., 2017). In this work, a high value of DS revealed to the high solubility of NdC-based CMC in water. For comparison, the commercial CMC provided by Sigma-Aldrich exhibited a DS value of 0.89. In line with this phenomenon, the DS analysis of NdC-based CMC was significantly impacted by the molecular interactions of NaOH and MCA. NaOH promoted the disintegration of cellulose's crystalline structure, hence increasing the accessibility of its molecules to replacement agents. MCA, on the other hand, acted as a replacing agent by adding carboxymethyl groups to cellulose to replace its hydroxyl groups. IR analysis provided information about the reaction mechanism, which was further supported by characterization of the diffraction pattern and evaluations of thermal degradation, as shown in Figure 7 (Shui et al., 2017; Wongvitvichot et al., 2021).

### 3.2.2 Analysis of Viscosity, Mw, and Final CMC Content

Viscosity denotes the extent of a fluid's resistance to unimpeded flow. Table 2 presented the viscosity values of NdC-based CMC and commercial Sigma-Aldrich CMC at a temperature of 25 °C. According to the viscosity values in Table 2, NdC-based CMC was classified as a low-viscosity, semi-purified CMC, rendering it more appropriate for application in oil and gas drilling muds (Mondal et al., 2015).

**Table 2.** Comparative Study of CMC's Viscosity

Parameter	Viscosity (mPa·s)	Reference
NdC-based CMC	25	This study
Sigma-Aldrich standard CMC	157	This study
Air particle vacuum dust-based CMC	90	(Çelikçi et al., 2022)
Mixed office waste-based CMC	76	(Joshi et al., 2015)
Cornstark-based CMC	16.24	(Shui et al., 2017)

Mw is a crucial quantity in polymer characterization, quantifying the average molecular weight by considering the weighted contributions of each molecule within a distribution. Molecular weight substantially influences the viscosity of CMC solutions. Polymers with elevated molecular weight typically yield increased viscosity, rendering them essential in applications including thickeners, stabilizers, and gel-forming agents. According to the Mw values in Table 3, the synthesized NdC-based CMC has a propensity for forming more stable solutions owing to enhanced molecular interactions.

**Table 3.** Comparative Study of CMC's Mw

Parameter	Mw (Da)	Reference
NdC-based CMC	2,075,165	This study
Sigma-Aldrich standard CMC	3,583,740	This study
Cornhusk-based CMC	2,558,967	(Mondal et al., 2015)
Office paper waste-based CMC	2,292,152	(Wongvitvichot et al., 2021)
Seaweed-based CMC	1,072,050	(Lakshmi et al., 2017)

The final content of NdC-based CMC signifies the purity of the resultant product. The analysis findings demonstrated that NdC-based CMC has a purity of 93.30%, as shown in Table 4. This indicated the existence of impurities in the NdC-based CMC, requiring additional treatment to attain a greater degree of purity.

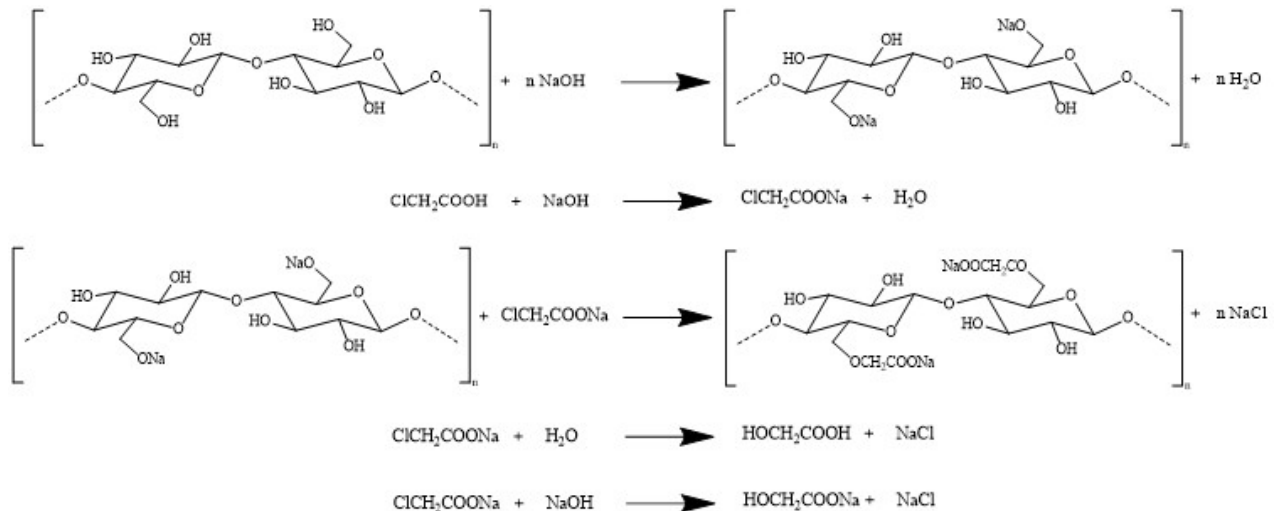


**Figure 7.** The Reaction Mechanism for the Formation of NdC-Based CMC

**Table 4.** Comparative Study of CMC's Purity

Parameter	Purity (%)	Reference
NdC-based CMC	83.30	This study
Sigma-Aldrich standard CMC	93.30	This study
Cornhusk-based CMC	99.99	(Mondal et al., 2015)
Mixed office waste-based CMC	150.80	(Joshi et al., 2015)
Hemp fiber-based CMC	96,96	(Duangrin et al., 2024)

**Table 5.** Comparative Study of CMC's WRC and ORC

Parameter	WRC (g.g <sup>-1</sup> )	ORC (g.g <sup>-1</sup> )	Reference
NdC-based CMC	3.90	2.20	This study
Sigma-Aldrich standard CMC	5.10	1.50	This study
Cornhusk-based CMC	5.11	1.59	(Mondal et al., 2015)
Agricultural waste-based CMC	3.81	1.66	((Singh et al., 2022)

### 3.2.3 Analysis of WRC and ORC

WRC denotes the capability of a material, such as a polymer, to absorb and keep water inside its internal structure without undergoing dissolution. WRC is scientifically linked to the hydrophilic characteristics of the material and the existence of polar functional groups, such as hydroxyl or carboxyl groups, which can engage with water molecules via hydrogen bonding. ORC refers to a material's capability to absorb and hold oil or fat inside its structure. This capacity is contingent upon the material's structural properties, including porosity and surface area, as well as its chemical affinity for oil. Table 5 presented data on the WRC and ORC values of NdC-based CMC. The findings revealed that NdC-based CMC primarily possesses hydrophilic characteristics, resulting from the substitution of hydroxyl groups with carboxymethyl groups via an etherification reaction (Mondal et al., 2015).

### 3.2.4 Analysis of Density and Color of NdC-Based CMC

Density denotes the compactness of atoms or molecules within a material. The density measurements for NdC-based CMC and commercial CMC from Sigma-Aldrich were determined

to be 1.002 g/mL and 1.0007 g/mL, respectively. These findings suggested that the NdC-based CMC has a density value comparable to the commercial CMC from Sigma-Aldrich.

Colorimetric analysis yields three parameters: L\*, a\*, and b\*. The L\* parameter in the CIE Lab\* color coordinate system denotes the brightness level of an object. The L\* scale extends from 0, denoting absolute black or the lack of reflected light, to 100, signifying pure white (maximum reflectance). The a\* parameter in the CIE Lab\* color coordinate system denotes the color dimension along the red-green axis, with a\* (+) indicating red dominance, a\* (-) indicating green dominance, and a\* = 0 signifying a neutral state with no substantial red or green component. In the CIE Lab\* color coordinate system, the b\* parameter symbolizes the color dimension along the blue-yellow axis, with b\* (+) indicating yellow dominance, b\* (-) indicating blue dominance, and b\* = 0 representing a neutral state with no major blue or yellow component. Table 6 displayed the outcomes of the color analysis for NdC-based CMC and commercial CMC sourced from Sigma-Aldrich. The results indicated that NdC-based CMC displays vibrant color attributes, closely identical to those of commercial CMC from Sigma-Aldrich, despite with minor impurities (Rachtanapun

et al., 2021).

**Table 6.** Analysis Results of CMC's Color

Parameter	L*	a*	b*
NdC-based CMC	80.69	5.39	10.56
Sigma-Aldrich standard CMC	91.24	3.15	7.02

### 3.2.5 Analysis of NaCl, Sodium Glycolate, and Heavy Metal Ions Content

NaCl and sodium glycolate are by-products generated during the manufacture of CMC via alkalization and carboxymethylation processes. The utilization of CMC as a food additive requires that the levels of NaCl and sodium glycolate, which are poisonous, be minimized. The presence of heavy metal ions, including Pb, Cd, Fe, and Cr, presents a contamination danger if found in high concentrations inside CMC. Table 7 displayed the analytical results for the amounts of NaCl, sodium glycolate, and heavy metal ions. The examination indicated that the concentrations of NaCl, sodium glycolate, and heavy metals (Pb, Cd, Fe, and Cr) in NdC-based CMC remain within acceptable limits, hence categorizing this product as semi-purified grade CMC.

**Synthesis and Characterization of CMC-Based Bioplastics**  
The fabrication of CMC-based bioplastics, utilizing both synthesized CMC and commercially sourced CMC from Sigma-Aldrich, was performed by the solvent casting technique. The synthesis outcomes were illustrated in Figure 8. The physical features of these bioplastics indicated that the CMC-based bioplastic from Sigma-Aldrich was flexible and translucent, but the synthesized CMC-based bioplastic was more rigid and less transparent. This signified that NdC-based CMC has been effectively converted into bioplastic, although with certain limitations, indicating the necessity for additional optimization investigation.

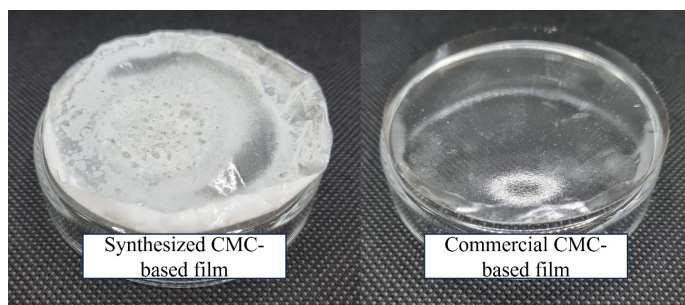


**Figure 8.** Bioplastics Produced from Synthesized and Commercial CMC

Additionally, the efficacy of the synthesis procedure for both bioplastics was evaluated utilizing IR spectroscopy and XRD diffraction patterns. Figure 9 displayed the infrared spectra of synthetic CMC-based bioplastics (Figure 9a) and commercial Sigma-Aldrich CMC (Figure 9b). All absorption bands in both

spectra displayed similarities to the infrared spectra of NdC-based CMC and commercial Sigma-Aldrich CMC depicted in Figure 2. The absorption at wavenumbers 3401–3344  $\text{cm}^{-1}$  was attributed to O–H stretching vibrations (Tavares et al., 2020). The absorption bands at 2922–2916  $\text{cm}^{-1}$  signified the asymmetric stretching vibrations of C–H in methylene groups (Tavares et al., 2020). The absorption bands at 1588–1585  $\text{cm}^{-1}$  corresponded to the vibrations of the carboxyl group ( $-\text{COO}^-$ ) (Tavares et al., 2020). The peaks at 1414  $\text{cm}^{-1}$  and 1322  $\text{cm}^{-1}$  were attributed to bending vibrations of  $-\text{CH}_2$  and C–H, respectively (Tavares et al., 2020). The absorption bands at 1020–1017  $\text{cm}^{-1}$  signified HOC–O– $\text{CH}_2$  stretching vibrations (Tavares et al., 2020).

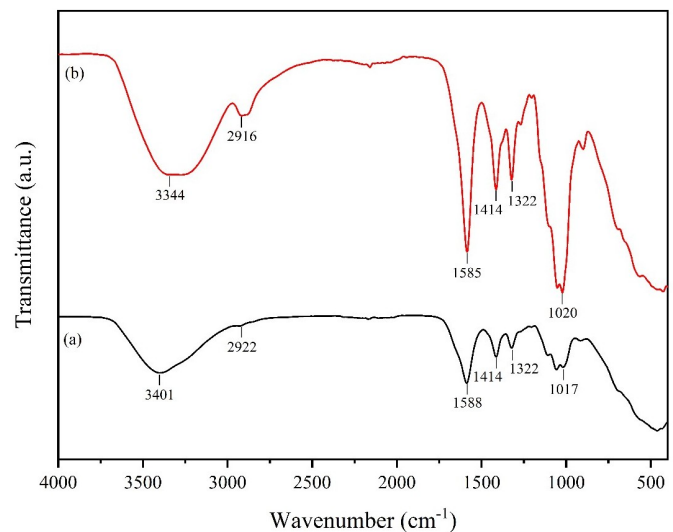


**Figure 9.** Infrared Spectra of Synthesized (a) and Commercial (b) CMC-Based Bioplastics

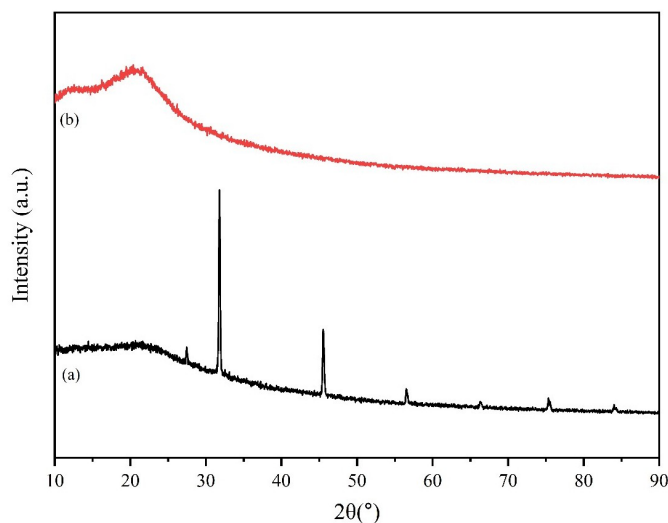
The XRD characterization results for bioplastics derived from synthetic CMC and commercial CMC from Sigma-Aldrich were illustrated in Figure 10. The diffraction pattern of bioplastics formed from synthesized CMC revealed an amorphous structure with minor crystalline peaks at  $2\theta$  angles of  $31.8^\circ$  and  $45.5^\circ$ , while bioplastics produced from commercial CMC by Sigma-Aldrich primarily demonstrated an amorphous character. This condition was believed to result from leftover cellulose crystals that were not completely destroyed during the alkalization and carboxymethylation processes in prior phases. Nonetheless, both diffraction patterns often display analogous properties, suggesting that bioplastics derived from synthetic CMC were comparable to those produced from commercial CMC by Sigma-Aldrich.

### 3.3 Physicochemical Analysis of Bioplastics

A physico-chemical examination of bioplastics derived from synthetic CMC and commercial CMC from Sigma-Aldrich was performed to assess many critical parameters, including TS, E, transmittance, water solubility, and biodegradability. Figure 11 displayed the test results for TS (blue) and E (green)

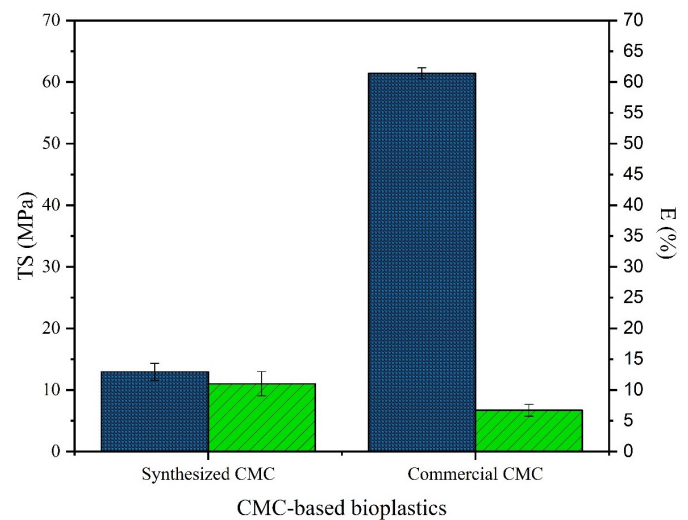
**Table 7.** Comparative Study of CMC's NaCl, Sodium Glycolate, and Heavy Metal Ions Content

Parameter	NaCl (%)	Sodium glycolate (%)	Heavy metal ions (ppm)				References
			Pb	Cd	Fe	Cr	
NdC-based CMC	0.55	0.038	1.07	Not detected	1.98	Not detected	This study
Sigma-Aldrich standard CMC	0.33	0.025	0.78	Not detected	0.31	0.97	This study
Cornhusk-based CMC	0.009	0.001	0.0005	0.001	Not provided	Not provided	(Mondal et al., 2015)

**Figure 10.** Diffraction Patterns of Synthesized (a) and Commercial (b) CMC-Based Bioplastics

of both categories of bioplastics. The TS values of bioplastics derived from synthetic CMC exhibited significant variation compared to those utilizing commercial CMC from Sigma-Aldrich, but the discrepancies in E values were less notable. The significant variations in TS suggested that bioplastics derived from synthetic CMC possess a stiff and less elastic physical nature. This was likely due to contaminants in the produced CMC from NdC, which restricted its optimal performance in bioplastic processing (Rachtanapun et al., 2021; Tavares et al., 2020).

In line with the findings of TS and E analysis, the produced bioplastics were characterized by their transmittance. Transmittance is an essential metric in assessing CMC-based bioplastics, especially for applications necessitating transparency, such as food packaging, coating films, or optical applications. The transmittance value denotes the quantity of light that can permeate the bioplastic, with elevated transmittance indicating enhanced transparency. The test findings indicated that the synthesized CMC-based bioplastic shown a transmittance value of 11.53%, while the commercial CMC-based bioplastic from Sigma-Aldrich revealed a transmittance value of 74.7%. The synthesized CMC-based bioplastic exhibits low transparency,

**Figure 11.** TS (blue) and E (green) of Synthesized and Commercial CMC-Based Bioplastics

presumably due to impurities, needing additional treatments to enhance its clarity (Rachtanapun et al., 2021).

This study also investigated the water solubility characteristics of both bioplastics. Water solubility is a critical factor in the utilization of bioplastics as food packaging materials, necessitating effective water resistance. The outcomes of the water solubility assessments indicated that both bioplastics rapidly dissolve in water. This was due to the elevated concentration of hydrophilic groups in the bioplastics, which quickly engage with water molecules during immersion assessments (Rachtanapun et al., 2021). Moreover, further research is necessary to integrate alternative modifying agents to diminish the water solubility of these bioplastics.

A crucial physicochemical measurement for evaluating bioplastics is the soil biodegradation test. This assessment measures the capacity of bioplastics to decompose into simpler substances, including water, carbon dioxide, methane, and other biomass, via the action of microorganisms (bacteria, fungi, or algae) under designated environmental circumstances. The test seeks to ascertain the degree and velocity of material decomposition in a soil environment. Figure 12 displayed the

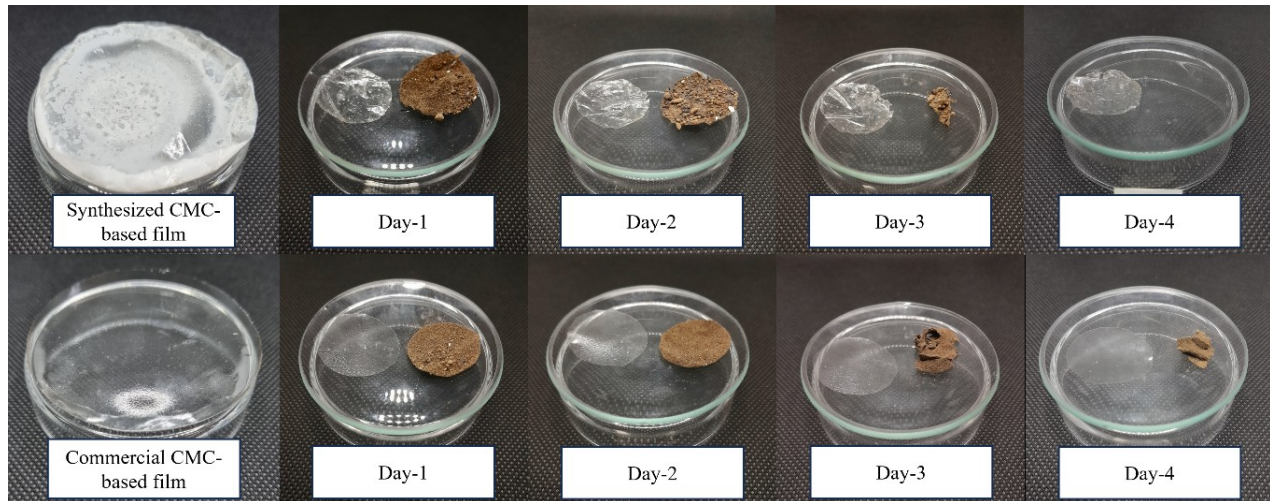


**Figure 12.** Biodegradation test of Synthesized and Commercial CMC-Based Bioplastics

outcomes of the biodegradation experiments for both bioplastics. Both bioplastics were degraded by fungi, especially *Trichoderma*, and other soil microorganisms, progressively breaking down from day 0 until complete degradation by day 4. The disintegration rate of the synthesized CMC-based bioplastic was marginally more rapid than that of the commercial CMC-based bioplastic from Sigma-Aldrich. The disparity was likely attributable to the inclusion of contaminants, such as cellulose crystals abundant in sugars sourced from DMCW, in the generated bioplastic, which may enhance microbial activity and expedite decomposition (Yaradoddi et al., 2020).

#### 4. CONCLUSIONS

The DMCW-derived NdC and NdC-derived CMC have been effectively produced via a technique that includes fermentation facilitated by the *Acetobacter xylinum* starter, subsequent alkali treatment, and carboxymethylation. Spectroscopic analysis, thermal testing, organoleptic assessment, proximate analysis, and physicochemical measurements confirmed the successful synthesis of DMCW-based NdC, NdC-based CMC, and CMC-based bioplastics. The NdC-based CMC derived from DMCW-based NdC demonstrated physicochemical features close to those of commercial CMC, positioning it as a possible precursor for bioplastic synthesis, despite existing limitations. In the future, CMC-based bioplastics, equipped with additional processing, have the potential to function as food packaging materials.

#### 5. ACKNOWLEDGMENT

KSR, AVN, EAP, VM, AR, and BI praise Allah Azza wa Jalla for the blessings and ease provided during the conceptualization, investigation, formal analysis, and writing–review and editing of this work and its paper. KSR, AVN, EAP, and VM express gratitude to the Research Program (Penelitian Dosen Pemula–PDP) for financial support for the 2024 fiscal

year, facilitated by the Directorate of Research, Technology, and Community Service (DRTPM Kemendikbudristek) under Main Contract number 108/E5/PG.02.00.PL/2024, along with Derivative Contract numbers 045/LL6/PB/AL.04/2024 and 606.4/PT/LPPM/VI/2024. KSR and BI dedicate this article to our daughter, Delisha Zelmira Aurum, on her second birthday. All authors thank CV. ARD Pratama for supplying high-quality pro-analysis grade chemicals for this study.

#### REFERENCES

- Aba, R. P. M., M. B. Z. Luna, J. C. Villasis, and A. A. A. Ching (2024). Characterization of Mature Coconut (*Cocos nucifera* L.) Water from Different Varieties. *Food and Humanity*, **2**; 100248
- Adinugraha, M. P., D. W. Marseno, and Haryadi (2005). Synthesis and Characterization of Sodium Carboxymethylcellulose from Cavendish Banana Pseudo Stem (*Musa cavendishii* Lambert). *Carbohydrate Polymers*, **62**(2); 164–169
- Alabi, F. M., L. Lajide, O. O. Ajayi, A. O. Adebayo, S. Emmanuel, and A. E. Fadeyi (2020). Synthesis and Characterization of Carboxymethyl Cellulose from *Musa paradisiaca* and *Tithonia diversifolia*. *African Journal of Pure and Applied Chemistry*, **14**(1); 9–23
- Andrade, M. S., O. H. Ishikawa, R. S. Costa, M. V. S. Seixas, R. C. L. B. Rodrigues, and E. A. B. Moura (2022). Development of Sustainable Food Packaging Material Based on Biodegradable Polymer Reinforced with Cellulose Nanocrystals. *Food Packaging and Shelf Life*, **31**; 100807
- Detudom, R., P. Deetae, H. Wei, H. Boran, S. Chen, S. Siri-amornpun, and C. Prakitchaiwattana (2023). Dynamic Changes in Physicochemical and Microbiological Qualities of Coconut Water During Postharvest Storage Under Different Conditions. *Horticulturae*, **9**(12); 1284
- Du, H., X. Sun, X. Chong, M. Yang, Z. Zhu, and Y. Wen (2023). A Review on Smart Active Packaging Systems for

- Food Preservation: Applications and Future Trends. *Trends in Food Science and Technology*, **141**; 104200
- Duangrin, M., S. Pisutpiched, A. Deenu, and S. Kamthai (2024). Ultrasonic-Assisted Synthesis for the Production of Green and Sustainable Hemp Carboxymethyl Cellulose. *International Journal of Biological Macromolecules*, **280**; 135610
- Ge, Y. and Z. Li (2013). Preparation and Evaluation of Sodium Carboxymethylcellulose from Sugarcane Bagasse for Applications in Coal-Water Slurry. *Journal of Macromolecular Science, Part A: Pure and Applied Chemistry*, **50(7)**; 757–762
- Halib, N., M. C. I. M. Amin, and I. Ahmad (2010). Unique Stimuli Responsive Characteristics of Electron Beam Synthesized Bacterial Cellulose/Acrylic Acid Composite. *Journal of Applied Polymer Science*, **116(5)**; 2920–2929
- Joshi, G., S. Naithani, V. K. Varshney, S. S. Bisht, V. Rana, and P. K. Gupta (2015). Synthesis and Characterization of Carboxymethyl Cellulose from Office Waste Paper: A Greener Approach Towards Waste Management. *Waste Management*, **38(1)**; 33–40
- Kong, X., Z. Guo, Y. Yao, L. Xia, R. Liu, H. Song, and S. Zhang (2022). Acetic Acid Alters Rhizosphere Microbes and Metabolic Composition to Improve Willows Drought Resistance. *Science of the Total Environment*, **844**; 157132
- Kumar, B., R. Priyadarshi, Sauraj, F. Deeba, A. Kulshreshtha, K. K. Gaikwad, J. Kim, A. Kumar, and Y. S. Negi (2020). Nanoporous Sodium Carboxymethyl Cellulose-g-Poly(Sodium Acrylate)/FeCl<sub>3</sub> Hydrogel Beads: Synthesis and Characterization. *Gels*, **6(4)**; 1–11
- Lakshmi, D. S., N. Trivedi, and C. R. K. Reddy (2017). Synthesis and Characterization of Seaweed Cellulose Derived Carboxymethyl Cellulose. *Carbohydrate Polymers*, **157**; 1604–1610
- Luo, H., T. Cui, D. Gan, M. Gama, Q. Zhang, and Y. Wan (2019). Fabrication of a Novel Hierarchical Fibrous Scaffold for Breast Cancer Cell Culture. *Polymer Testing*, **80**; 106107
- Mondal, M. I. H., M. S. Yeasmin, and M. S. Rahman (2015). Preparation of Food Grade Carboxymethyl Cellulose from Corn Husk Agrowaste. *International Journal of Biological Macromolecules*, **79**; 144–150
- Nimeskern, L., H. Martínez Ávila, J. Sundberg, P. Gatenholm, R. Müller, and K. S. Stok (2013). Mechanical Evaluation of Bacterial Nanocellulose as an Implant Material for Ear Cartilage Replacement. *Journal of the Mechanical Behavior of Biomedical Materials*, **22**; 12–21
- Phan, H. T., K. D. Nguyen, H. H. M. Nguyen, N. T. Dao, P. T. K. Le, and H. V. Le (2023). Nata de Coco as an Abundant Bacterial Cellulose Resource to Prepare Aerogels for the Removal of Organic Dyes in Water. *Bioresource Technology Reports*, **24**; 101613
- Rachtanapun, P., P. Jantrawut, W. Klunklin, K. Jantanasakulwong, Y. Phimolsiripol, N. Leksawasdi, P. Seesuriyachan, T. Chaياسo, C. Insomphun, S. Phongthai, S. R. Sommano, W. Punyodom, A. Reungsang, and T. M. P. Ngo (2021). Carboxymethyl Bacterial Cellulose from Nata de Coco: Effects of NaOH. *Polymers*, **13(3)**; 1–17
- Rahmasari, K. S. and B. Ishartono (2024). Antioxidant Release Profile from Chitosan/k-Carrageenan-Based Polyelectrolyte Complex Films as Active Packaging: A Preliminary Study. *Molekul*, **19(3)**; 443–454
- Rahmatullah, R. W. Putri, M. Rendana, U. Waluyo, and T. Andrianto (2022). Effect of Plasticizer and Concentration on Characteristics of Bioplastic Based on Cellulose Acetate from Kapok (*Ceiba pentandra*) Fiber. *Science and Technology Indonesia*, **7(1)**; 73–83
- Ramakrishnan, R., J. T. Kim, S. Roy, and A. Jayakumar (2024). Recent Advances in Carboxymethyl Cellulose-Based Active and Intelligent Packaging Materials: A Comprehensive Review. *International Journal of Biological Macromolecules*, **259**
- Roslan, N. J., S. H. Jamal, J. I. A. Rashid, M. N. F. Norrahim, K. K. Ong, and W. M. Z. W. Yunus (2024). Response Surface Methodology for Optimization of Nitrocellulose Preparation from Nata de Coco Bacterial Cellulose for Propellant Formulation. *Heliyon*, **10(4)**; e25993
- Saputra, A. H., L. Qadhaiyna, and A. B. Pitaloka (2014). Synthesis and Characterization of Carboxymethyl Cellulose (CMC) from Water Hyacinth Using Ethanol-Isobutyl Alcohol Mixture as the Solvents. *International Journal of Chemical Engineering and Applications*, **5(1)**; 36–40
- Shui, T., S. Feng, G. Chen, A. Li, Z. Yuan, H. Shui, T. Kuboki, and C. Xu (2017). Synthesis of Sodium Carboxymethyl Cellulose Using Bleached Crude Cellulose Fractionated from Cornstalk. *Biomass and Bioenergy*, **105**; 51–58
- Singh, R., J. Singh, Sonika, and H. Singh (2022). Green Synthesis of Carboxymethyl Cellulose from Agricultural Waste Its Characterization. *Journal of Physics: Conference Series*, **2267(1)**; 1–18
- Tavares, K. M., A. d. Campos, B. R. Luchesi, A. A. Resende, J. E. d. Oliveira, and J. M. Marconcini (2020). Effect of Carboxymethyl Cellulose Concentration on Mechanical and Water Vapor Barrier Properties of Corn Starch Films. *Carbohydrate Polymers*, **246**; 116521
- Techavuthiporn, C., H. Nimitkeatkai, M. Thammawong, and K. Nakano (2024). A Coating Made from Carboxymethyl Cellulose Derived from Commercial Nata De Coco Reduces Postharvest Changes in ‘Hom Thong’ Banana Fruit During Ambient Storage. *Postharvest Biology and Technology*, **208**; 112650
- Wongvitvichot, W., S. Pithakratanayothin, S. Wongkasemjit, and T. Chaisuwan (2021). Fast and Practical Synthesis of Carboxymethyl Cellulose from Office Paper Waste by Ultrasonic-Assisted Technique at Ambient Temperature. *Polymer Degradation and Stability*, **184**; 109473
- Yaradoddi, J. S., N. R. Banapurmath, S. V. Ganachari, M. E. M. Soudagar, N. M. Mubarak, S. Hallad, S. Hugar, and H. Fayaz (2020). Biodegradable Carboxymethyl Cellulose Based Material for Sustainable Packaging Application. *Scientific Reports*, **10(1)**; 21960
- Youssif, A. A. A. and M. T. Hassan (2018). Synthesis and Characteristic of Carboxymethyl Cellulose from Baobab (*Adansonia digitata* L.) Fruit Shell. *International Journal of*

*Engineering and Applied Sciences (IJEAS)*, 5(12); 1–10  
Çelikçi, N., C. A. Ziba, and M. Dolaz (2022). Synthesis and Characterization of Carboxymethyl Cellulose (CMC) from Different Waste Sources Containing Cellulose and Inves-

tigation of Its Use in the Construction Industry. *Cellulose Chemistry and Technology*, 56(1–2); 55–68